

Evaluation of Mechanical Behavior of 3D Printed Lattice Structure by SLM: Experiment and FEA

VRÁNA Radek^{1,a}, VOSYNEK Petr^{1,b}, KOUTNÝ Daniel^{1,c},
NÁVRAT Tomáš^{1,d} and PALOUŠEK David^{1,e}

¹Faculty of Mechanical Engineering, Brno University of Technology,
Technická 2896/2, 616 69 Brno, Czech Republic

^avrana@fme.vutbr.cz, ^bvosynek@fme.vutbr.cz, ^cnavrat@fme.vutbr.cz, ^ekoutny@fme.vutbr.cz,
^dpalousek@fme.vutbr.cz

Keywords: selective laser melting, additive manufacturing, material properties, lattice structure.

Abstract. This paper deals with the prediction of the mechanical behaviour of lattice structures made by selective laser melting (SLM). The work was divided into two stages where the first was aimed on evaluation of the material model for finite element analysis (FEA) from proposed tensile test specimens. The second stage was using previously evaluated material model for more complex structures composed of periodical truss cells. It was found that the major issue was the real geometry of additively produced specimens. For evaluation, stress-strain diagrams were used. All manufactured parts were made of aluminium alloy AlSi10Mg.

Introduction

Selective laser melting (SLM) is layer by layer additive manufacturing (AM) method which allows creating objects with a complex shape that are very difficult to produce by conventional technologies. There are many great examples in nature, e.g. bone tissue composition - trabecular bone and osteons in compact bone, both oriented in the direction of principal stresses [1] or internal structure of plants such as bamboo.

The general shape such as bone or bamboo is very difficult to create in 3D software, therefore general shape is replaced by the lattice structure with periodically repeating unit shape in engineering [2]. Due to high strength to weight ratio and good energy absorption capacity, Body Centred Cubic (BCC) shape of lattice structure is very popular [3].

Mechanical properties of the SLM parts are strongly dependent on used laser process parameters of the technology. It is clearly shown in the articles [3, 4, 5], where authors present influence of three main parameters – laser speed (LS), laser power (LP) and laser hatch distance (HD) on material and mechanical properties of aluminium alloys. Many authors describe mechanical properties of a bulk material in tension, e.g. Kempen et. al. [6] describes different mechanical properties in XY and Z direction due to elongation at break which is caused by porosity close to the part surface. If we consider a lattice structure formed by thin trusses, this close to surface porosity can greatly decrease the mechanical properties of each truss in the structure. The other authors also found out that the shape of parts and then also mechanical properties in lattice structure are dependent on building direction and surface roughness [7, 8].

Based on these studies, the methodology for obtaining a material model of BCC lattice structure material for FEA analysis was created.

Materials and methods

Additive manufacturing. All samples were made of aluminum powder AlSi10Mg by the SLM 280^{HL}, the metal additive technology machine with building space 280x280x350 mm³. The device allows producing parts from many types of metal powder materials (aluminum alloys, titanium alloys, stainless steel, etc.). The metal powder is melted by YLR-Laser with a power of 400W [9]. During the production, there is the inert atmosphere N₂ and Ar inside the build chamber. Therefore, the device can be used even for very reactive materials.

Tensile Specimens. All tensile specimens were produced with a default setting for the AlSi10Mg material and added with a cooling delay of each layer (15 seconds) before production of next layer. Samples were not further modified (heat treatment or surface finishing). To capture the effect of size (truss diameter: 0.45 mm, 1 mm) and different building angle (90°, 45°) [3], four groups of five pieces were made. Samples of different groups have the same total area of cross-section for the purpose of comparison the mechanical parameters.

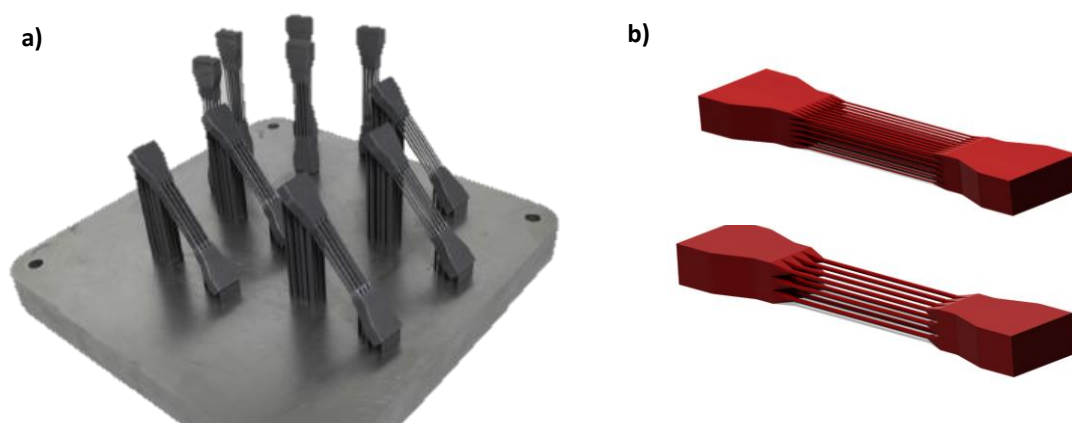


Fig. 1(a) Specimens for tensile tests on the platform after manufacturing by SLM 280HL; (b) CAD models of the tensile specimens

Compression Specimens. All compression samples were sandwich blocks 20x20x20 mm³ of BCC lattice structure with the bottom and upper plate ($t = 0.3$ mm). A unit cell was composed of eight trusses with nominal diameter $d = 0.5$ mm and its dimensions were 4x4x4 mm³. It results that every layer was created by 5x5 unit cells. All compression samples were also manufactured with the default setting for AlSi10Mg material and not further modified (heat treatment or surface finishing).

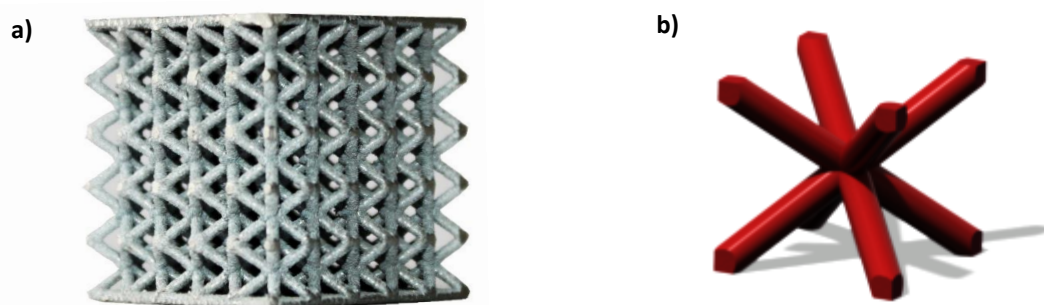


Fig. 2 (a) Specimens for compression tests manufactured by SLM 280HL; (b) CAD model of the BCC unit cell

Quality and surface roughness. The tensile samples were digitized in the as-built state on the ATOS Triple Scan. The acquired 3D geometry of the real trusses was analyzed in the GOM Inspect software, to find the difference between design and real geometry. For better quality of measurement, the surface of the samples was mated with titan powder [10].

Mechanical testing. In order to get an information about the mechanical behavior of the manufactured structures, a tensile and compressive test were performed. For the mechanical testing universal testing machine, ZWICK Z020 was used.

FEA. For the purpose of the further design of 3D printed lattice structures, the computational model was made. Ideal geometry was first considered and further corrected for the deviation of the real trusses delivered from the 3D scanner. To simulate the behavior of the tensile test in the elastic-plastic region, nonlinear model of material needs to be involved in FEA. The bilinear behavior was chosen. The parameters of the bilinear model of material were iteratively modified to ultimately match the tensile test stress-strain diagram.

Results and analysis

Tensile experiments. The tensile test results show the different deformation behavior of the produced samples (Fig. 3a), when design dimensions were used for evaluation. The results are divided into the two regions according to the diameter of the trusses. Due to the same nominal area of the cross-section, this division should not have occurred. To eliminate this effect, real diameters obtained by optical measurement were applied. There were significant differences between design and real diameter and between 45° and 90° manufacturing orientation. For the design diameter $d_1 = 0.45$ mm with manufacturing orientation 90°, the real diameter $d_1' = 0.64$ mm were evaluated. For orientation 45°, the real diameter was $d_2' = 0.66$ mm. The same effect with smaller deviation was observed for design diameter $d_3 = 1.00$ mm. The real diameter $d_3' = 1.04$ mm for 90° and $d_4' = 1.05$ mm for 45° orientation were evaluated. The results after the correction are more consistent and the differences in the linear region of the stress-strain diagram are small (Fig.3b).

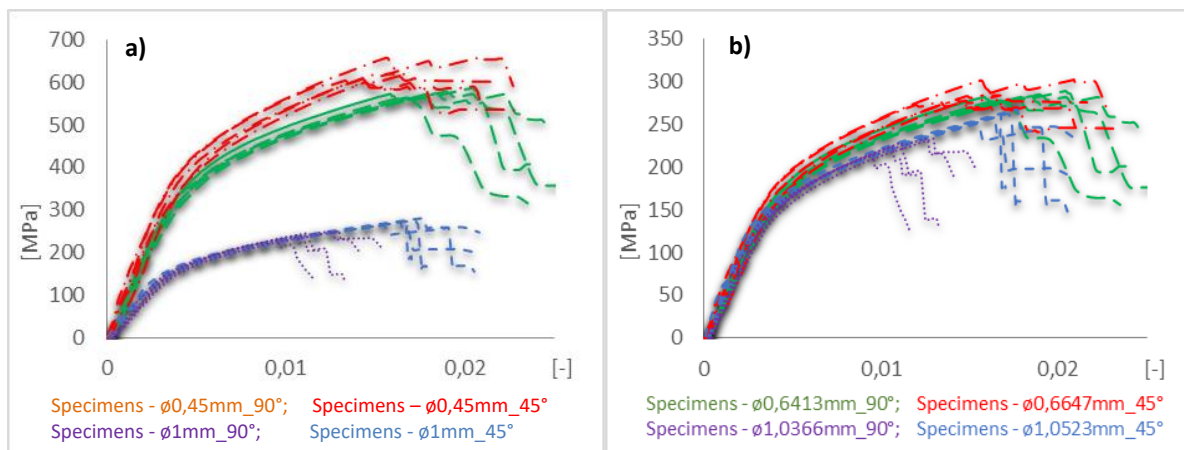


Fig. 3 (a) Tensile test evaluation with design diameters; (b) Tensile test evaluation with real diameters

Tensile simulations. Based on the experimental data, the bilinear model of material was evaluated for trusses with nominal diameter 0.45 mm and orientation 45°. Such set up is the closest to the dimensions and building orientation for BCC lattice structure which was planned to be tested afterward. Geometry was discretized by the tetrahedral quadratic elements. The model of material parameters was at this stage: Young modulus $E = 49$ GPa,

yield strength $R_{p0,2} = 211$ MPa, tangent modulus $E_T = 12.1$ GPa (evaluated according to equations 1-4) and Poisson's ratio $\mu = 0.33$. The simulation set up was following the tensile testing with the correction on real beams geometry. After nonlinear solution, the stress-strain diagram was compared with experimental data (fig.4).

$$R_m = E_T \cdot (\varepsilon_m - \varepsilon_{el}) + R_e \quad (1)$$

$$E_T = \frac{R_m - R_e}{\varepsilon_m - \varepsilon_{el}} \quad (2)$$

$$\varepsilon_{el} = \frac{R_e}{E} = \frac{211}{49000} = 0.00431 \quad (3)$$

$$E_T = \frac{280 - 211}{0.01 - 0.00431} = 12118 \text{ MPa} \quad (4)$$

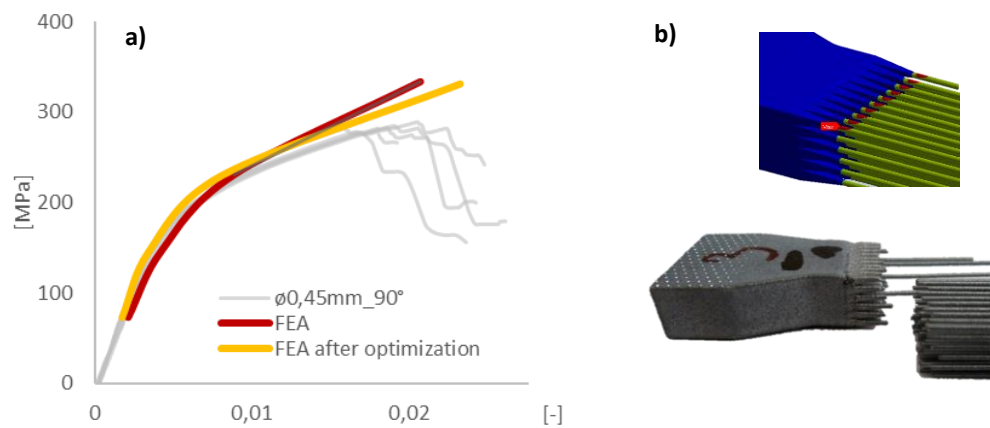


Fig. 4 (a) Stress-strain diagram after non-linear solution; (b) The results of the non-linear solution compared to real failure

The difference is probably caused by other uncertainties which are typical for the SLM technology. It is mainly high surface roughness due to the partial melting of the surrounding metal powder. This rough surface can easily initiate the crack. The second main uncertainty is the porosity and it's weakening of the cross-section area [6]. To correct the difference in stress-strain dependencies, Young modulus and tangent modulus were modified (fig.4a): $E = 60$ GPa, $E_T = 9.4$ GPa. All other measured mechanical properties are shown in fig. 5 (default settings for boxplots were used in Minitab software).

Compression experiments. During the compression, the individual layers are gradually deformed and densification of lattice structure material occurs. Such behavior is seen on the force-deformation dependency, where the compression load rapidly decreases and then increases after the first collapse (fig. 6a). The main objective of our study is to predict the mechanical behavior of lattice structure made of AlSi10Mg up to the first irreversible collapse, by setting up correctly the model of material in our FEA analysis.

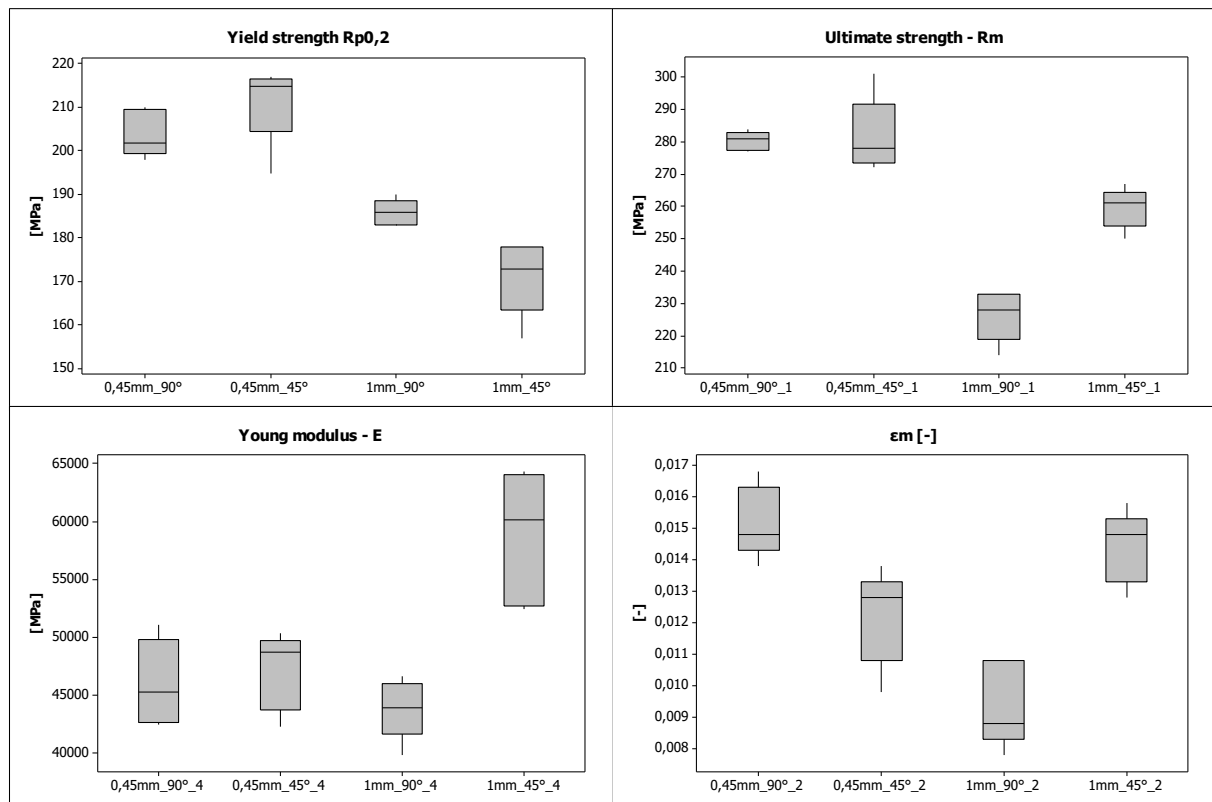


Fig. 5 Box plots of the measured mechanical parameters

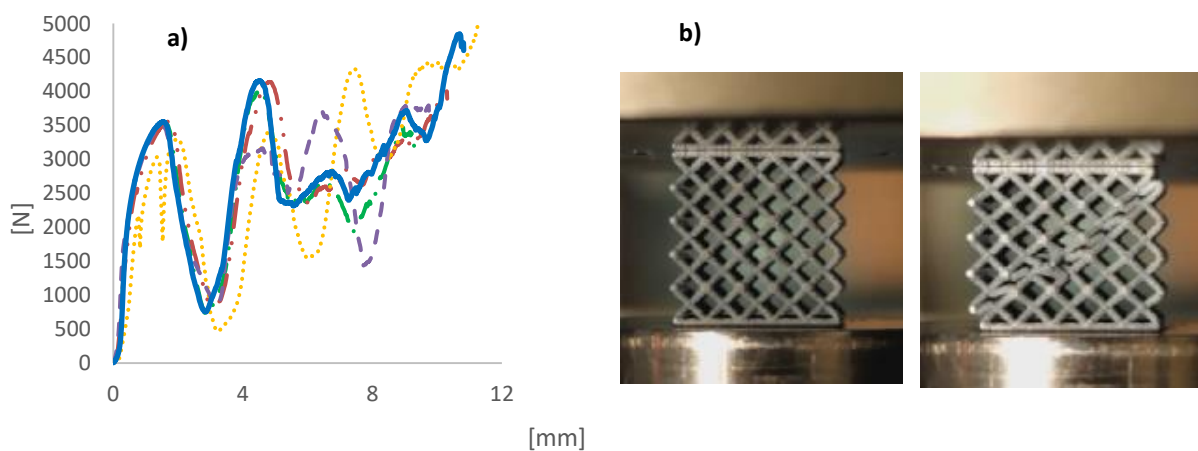


Fig. 6 (a) Force – deformation compression test data with design diameters; (b) Real deformation of the lattice structure

Compression simulations. To validate the obtained material model, a static load simulation of the lattice structure was performed. As before, in the case of tensile specimens, the surface of samples was optically digitized to obtain real dimensions. Based on dimensional analysis, the diameters were corrected from $d = 0.5$ mm to $d' = 0.72$ mm. With these diameters, the volumetric geometry of the structure was imported to ANSYS Workbench. Geometry was discretized by the tetrahedral quadratic elements. The size of the elements has been chosen so that there are at least three elements across the cross-section area. The simulation set up was following the compression testing with the correction on real beams geometry, with the same clamping and loading. Fig 7.

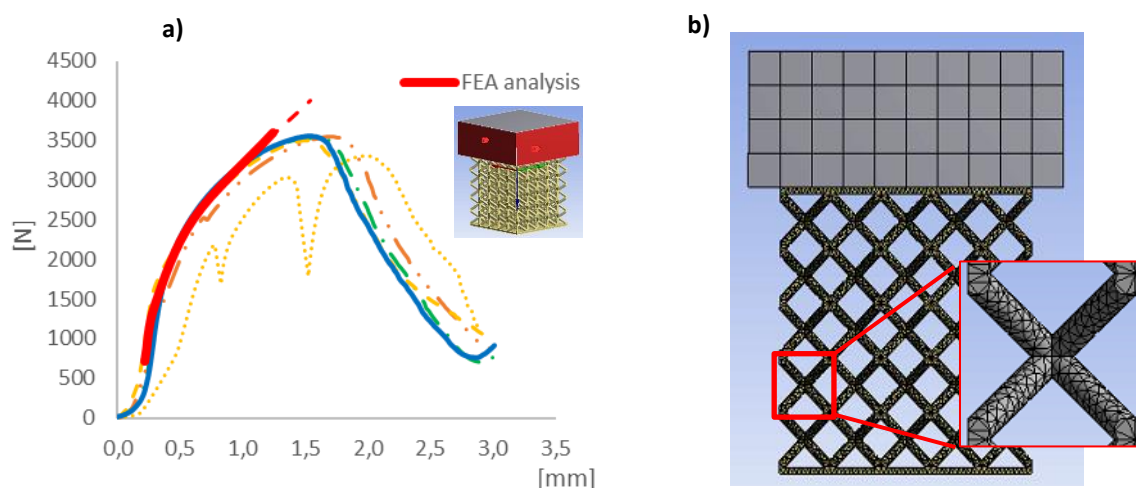


Fig. 7 (a) Force – deformation compression test data with design diameters and boundary conditions; (b) discretization of the geometry

Conclusion

Mechanical testing and computational modelling were used for the evaluation of the material behavior of lattice structures made by SLM machine SLM 280^{HT}. The main outputs of the work are: 1) material parameters (Young's modulus, strength, yielding stress, tangent modulus); 2) geometric correction for the deviation between the designed and real beams.

Acknowledgment

This work is an output of cooperation between project FSI-S-17-4144 and NETME Centre, regional R&D centre built with the financial support from the Operational Programme Research and Development for Innovations within the project NETME Centre (New Technologies for Mechanical Engineering), Reg. No. CZ.1.05/2.1.00/01.0002 and, in the follow-up sustainability stage, supported through NETME CENTRE PLUS (LO1202) by financial means from the Ministry of Education, Youth and Sports under the „National Sustainability Programme I”.

References

- [1] J. Šmarda. *Biologie pro psychology a pedagogy*. Vyd. 2. Praha: Portál, 2007, 420 s. ISBN 978-80-7367-343-7.
- [2] R. Vrána, D. Koutný, D. Paloušek. Impact Resistance of Different Types of Lattice Structures manufactured by SLM. *MM Science Journal*, 2016, roč. 2016, č. 6, s. 1579-1585. ISSN: 1803-1269.
- [3] LI, P., Z. Wang, N. Petrinic, C.R. Siviour. Deformation behaviour of stainless steel microlattice structures by selective laser melting. *Materials Science and Engineering: A* [online]. 2014, 614, 116-121 [cit. 2018-04-21]. DOI: 10.1016/j.msea.2014.07.015. ISSN 09215093.
- [4] D. Koutny, D. Palousek, L. Pantelejev. Ch. Hoeller, R. Pichler, L. Tesicky, J. Kaiser. Influence of Scanning Strategies on Processing of Aluminum Alloy EN AW 2618 Using

- Selective Laser Melting. *Materials* [online]. 2018, 11(2), 298- [cit. 2018-04-21]. DOI: 10.3390/ma11020298. ISSN 1996-1944.
- [5] D. Palousek, L. Pantelejev, T. Zikmund, D. Koutny. PROCESSING OF NEARLY PURE IRON USING 400W SELECTIVE LASER MELTING – INITIAL STUDY. *MM Science Journal* [online]. 2017, 2017(01), 1738-1743 [cit. 2018-04-21]. DOI: 10.17973/MMSJ.2017_02_2016184. ISSN 18031269.
- [6] K., L. Kempen, J. Thijs, van Humbeeck, J.-P. Kruth. Mechanical Properties of AlSi10Mg Produced by Selective Laser Melting. *Physics Procedia*. 2012, vol. 39, s. 439-446. DOI: 10.1016/j.phpro.2012.10.059. <http://linkinghub.elsevier.com/retrieve/pii/S1875389212025862>
- [7] M. Suard, P. Lhuissier, R. Dendievel, F. Vignat. Impact of EBM Fabrication Strategies on Geometry and Mechanical Properties of Titanium Cellular Structures. *Fraunhofer Direct Digital Manufacturing Conference*. 2014.
- [8] D. Koutný, R. Vrána, D. Paloušek. Dimensional accuracy of single beams of AlSi10Mg alloy and 316L stainless steel manufactured by SLM. In *5th International Conference on Additive Technologies iCAT2014*. Ljubljana: Interesansa, 2014. s. 142-147. ISBN: 978-961-281-579-0
- [9] Laser Beam Melting System SLM 280 HL. SLM SOLUTIONS GMBH. SLM Solutions GmbH [online]. [cit. 2014-05-16]. <http://stage.slmsolutions.com/download.php?f=61008aff89ca6259285ee7f35052f942>
- [10] D. Palousek, M. Omasta, D. Koutny, J. Bednar, T. Koutecky, F. Dokoupil. Effect of matte coating on 3D optical measurement accuracy. *Optical Materials* [online]. 2015, 40, 1-9 [cit. 2018-04-21]. DOI: 10.1016/j.optmat.2014.11.020. ISSN 09253467.